

# Anion-Dependent Facile Route to Magnetic Dinuclear and Dodecanuclear Cobalt Clusters

Ling-Ling Zheng,<sup>[a]</sup> Ji-Dong Leng,<sup>[a]</sup> Radovan Herchel,<sup>[b]</sup> Yan-Hua Lan,<sup>[c]</sup>  
Annie K. Powell,<sup>[c]</sup> and Ming-Liang Tong\*<sup>[a]</sup>

**Keywords:** Azides / Cobalt / Cluster compounds / Magnetic properties

An unprecedented dodecanuclear  $\text{Co}^{\text{III}}_3\text{Co}^{\text{II}}_9$  and a dinuclear  $\text{Co}^{\text{II}}_2$  cluster were synthesized facily from reactions of different cobalt(II) salts with the ligand (1*H*-benzimidazol-2-yl)-methanol. The cobalt ions in the  $\text{Co}_{12}$  supercluster are linked into a disclike structures through  $\mu_3\text{-O}_L$ ,  $\mu\text{-O}_L$ ,  $\mu_3\text{-O}^{2-}$ ,  $\mu_{1,1}\text{-N}_3^-$  and  $\mu_{1,1,1}\text{-N}_3^-$  bridges. Magnetic studies reveal that strong

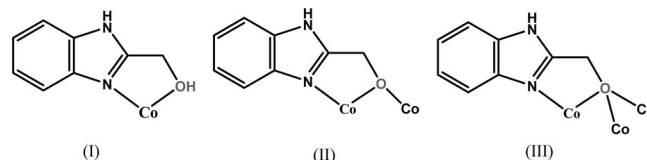
ferromagnetic coupling through double end-on (EO) azido bridges exists in **1**, while both ferromagnetic coupling through the  $\mu_3\text{-O}_L$  and  $\mu\text{-O}_L$  pathways and antiferromagnetic coupling through the  $\mu_{1,1,1}\text{-N}_3^-$  pathway exist in **2**, which results in a ferrimagnetic behaviour of **2**.

## Introduction

The design and synthesis of novel polynuclear clusters has become one of the most active areas in coordination chemistry,<sup>[1]</sup> since transition-metal clusters can show versatile magnetic behaviour,<sup>[2]</sup> in particular, they may exhibit single-molecule magnet (SMM) behaviour, and have potential application in information storage and quantum tunneling of magnetization.<sup>[3–7]</sup> The slow relaxation of magnetization is governed by the combination of a high-spin ground state  $S_T$  and uniaxial anisotropy  $D$ .

Manganese(III), iron(II,III), and cobalt(II) ions are good candidates for constructing SMMs because of their significant magnetic anisotropy. However, compared with the widely documented polynuclear  $\text{Mn}^{\text{III}}$  or  $\text{Fe}^{\text{III}}$  clusters, only a few iron(II) and cobalt(II) clusters have been investigated,<sup>[8]</sup> which may be ascribed to the absence of a facile synthesis route that prevents the  $\text{Fe}^{\text{II}}$  and  $\text{Co}^{\text{II}}$  ions from oxidation in air and to the challenge in controlling the magnetic coupling. Previous research indicates that hydroxy-containing ligands can hold metal ions together through the  $\mu_3\text{-O}$  bridging mode to transmit ferromagnetic interactions, which may cause the metal ion to be in a high-spin ground

state.<sup>[9]</sup> We have used amino alcohol ligands, such as triethanolamine (teaH<sub>3</sub>) and *N,N,N',N'*-tetrakis(2-hydroxyethyl)ethylenediamine (edteH<sub>4</sub>), to prepare a novel  $\text{Cu}_{17}\text{Mn}_{28}$  cluster with  $S_T = 51/2$  ground spin state and  $\text{Mn}_{12}$  clusters with tunable oxidation states,  $\text{Mn}^{\text{III}}_x\text{Mn}^{\text{II}}_{12-x}$  ( $x = 8, 10$  and  $12$ ).<sup>[10]</sup> Inspired by previous work, we extended our study to the cluster chemistry of 2-benzimidazolemethanol (HL) (Scheme 1), which is not well explored, and only few clusters based on HL have been reported.<sup>[11]</sup> The azide group has proven to be one of the most effective ligands in magnetic coupling pathways in polynuclear magnetic clusters.<sup>[12]</sup> Herein, we report two novel cobalt clusters isolated from the reactions of  $\text{Co}^{\text{II}}$  salts with HL and  $\text{NaN}_3$ , namely,  $[\text{Co}^{\text{II}}_2(\mu_{1,1}\text{-N}_3)_2(\text{HL})_4](\text{NO}_3)_2$  (**1**) and  $[\text{Co}^{\text{II}}_9\text{Co}^{\text{III}}_3(\mu_3\text{-O})_3(\mu_{1,1,1}\text{-N}_3)(\mu_{1,1}\text{-N}_3)_3(\mu_3\text{-L})_9(\mu\text{-L})_6](\text{ClO}_4)_2\cdot\text{H}_3\text{tea}\cdot 9.5\text{H}_2\text{O}$  (**2**). Three kinds of coordination modes of HL, chelate (I),  $\mu\text{:}\eta^1\text{:}\eta^2$  (II) and  $\mu_3\text{:}\eta^1\text{:}\eta^3$  (III), are found in **1** and **2** (Scheme 1), and the azide groups act as the  $\mu_{1,1}$  (in **1**) and  $\mu_{1,1,1} + \mu_{1,1}$  (in **2**) end-on bridges, respectively.



Scheme 1. The coordination modes of the HL ligand in **1** and **2**.

## Results and Discussion

Reaction of  $\text{Co}(\text{NO}_3)_2\cdot 6\text{H}_2\text{O}$  with HL and  $\text{NaN}_3$  in  $\text{CH}_3\text{OH}$  generates the dinuclear cobalt(II) complex  $[\text{Co}_2(\text{HL})_4(\text{N}_3)_2](\text{NO}_3)_2$  (**1**), while a novel disclike dodecanuclear  $\text{Co}^{\text{II}}_9\text{Co}^{\text{III}}_3$  cluster **2** was isolated from the above

[a] Key Laboratory of Bioinorganic and Synthetic Chemistry of Ministry of Education/State Key Laboratory of Optoelectronic Materials and Technologies, School of Chemistry and Chemical Engineering, Sun Yat-Sen University, Guangzhou 510275, P. R. China  
Fax: +86-20-8411-2245  
E-mail: tongml@mail.sysu.edu.cn

[b] Department of Inorganic Chemistry, Faculty of Science, Palacky University, tř. 17. listopadu 12, 77146 Olomouc, Czech Republic

[c] Institut für Anorganische Chemie der Universität Karlsruhe, Engesserstrasse Geb. 30.45, 76128 Karlsruhe, Germany

Supporting information for this article is available on the WWW under <http://dx.doi.org/10.1002/ejic.201000222>.

reaction, with the exception that  $\text{Co}(\text{NO}_3)_2 \cdot 6\text{H}_2\text{O}$  was replaced by  $\text{Co}(\text{ClO}_4)_2 \cdot 6\text{H}_2\text{O}$ , which shows that the final products are highly anion dependant. Moreover, when  $\text{NaN}_3$  was replaced by triethylamine, another interesting disclike  $\text{Co}_7$  cluster was obtained,<sup>[13]</sup> which indicates the effect of the type of base on the products.

X-ray crystal structure analysis reveals that the asymmetric unit of **1** consists of one half of the formula (Figure 1). Each neutral HL ligand is chelated to one cobalt(II) ion (Scheme 1). The  $\text{Co}^{\text{II}}$  adopts a distorted  $\text{N}_4\text{O}_2$  octahedral environment and is surrounded by two bidentate HL ligands and two azide anions with the  $\text{Co-N/O}$  bond lengths in the range 2.0716–2.2099 Å. Both the  $\text{Co1-N}_{\text{azido}}\text{-Co1a}$  angle  $[99.6(1)^\circ]$  and the  $\text{Co1}\cdots\text{Co1a}$  distance  $[3.213(3) \text{ Å}]$  are in the typical range for double EO-bridged compounds.<sup>[14]</sup> Adjacent dinuclear  $[\text{Co}_2(\mu_{1,1}\text{-N}_3)_2(\text{HL})_4]^{2+}$  cations and nitrate anions are linked into a 3D supramolecular architecture (see Figure S1 in the Supporting Information) through  $\text{N-H}\cdots\text{O}$  and  $\text{O-H}\cdots\text{O}$  hydrogen-bonding interactions  $[\text{N2}\cdots\text{O3}, 2.939(3) \text{ Å}; \text{O2}\cdots\text{O1}, 2.690(3) \text{ Å}]$ .

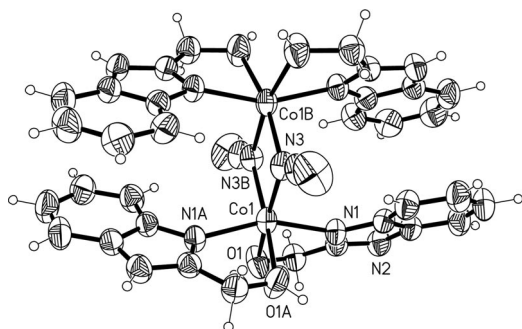


Figure 1. ORTEP drawing of the dinuclear cation in **1** with ellipsoids at the 50% probability level. Symmetry codes: (a)  $x, -y + 1/2, -z + 1/2$ ; (b)  $-x, -y + 1/2, z$ .

Compound **2** crystallizes in the trigonal space group  $P\bar{3}1c$  and contains a mixed-valence dodecanuclear complex with  $C_3$  symmetry (Figure 2). The asymmetric unit of the cation contains four independent cobalt ions ( $\text{Co1}$ ,  $\text{Co2}$ ,  $\text{Co3}$  and  $\text{Co4}$ ), five deprotonated  $\text{L}^-$  ligands, two  $\text{N}_3^-$  groups and one  $\text{O}^{2-}$  group. The central three cobalt ions ligated by  $\text{NO}_5$  donor atoms are divalent with  $\text{Co-O/N}$  bond lengths of 2.032–2.255 Å; moreover, six outer cobalt ions, which occupy the  $\text{N}_2\text{O}_4$  coordination sphere ( $\text{Co-N/O}$ , 2.012–2.258 Å) also are divalent. The remaining three outer cobalt ions that possess a  $\text{N}_3\text{O}_3$  ligand donor set ( $\text{Co-N/O}$ , 1.903–1.964 Å) are trivalent. Oxidation states have been assigned on the basis of bond valence sum analysis and consideration of bond lengths and charge balance.<sup>[15]</sup> The  $\text{Co}^{\text{II}}$  and  $\text{Co}^{\text{III}}$  ions are in a pseudo-octahedral coordination environment. The central three  $\text{Co1}$  ions are linked to each other by a  $\mu_{1,1,1}$ -azido bridge and  $\text{O}^{2-}$  bridges with a  $\text{Co}\cdots\text{Co}$  distance of 3.206 Å. The central  $\text{Co1}$  atom connects to the outer  $\text{Co2}$  ions through a  $\mu_3\text{-O}$  bridge and  $\text{O}^{2-}$  ( $\text{Co}\cdots\text{Co}$ , 3.148 Å). The  $\text{Co1}$  atom links the outer  $\text{Co3}$  and  $\text{Co4}$  atoms through two  $\mu_3\text{-O}$  bridges ( $\text{Co}\cdots\text{Co}$ , 3.140–3.216 Å). The outer  $\text{Co2}$  and  $\text{Co4}$  atoms are interlinked through a EO-azido bridge and a  $\mu_3\text{-O}$  bridge of  $\text{L}$  with a

$\text{Co}\cdots\text{Co}$  distance of 3.218 Å, but the  $\text{Co3}$  and  $\text{Co4}$  atoms are held together by  $\mu\text{-O}$  and  $\mu_3\text{-O}$  bridges ( $\text{Co}\cdots\text{Co}$ , 3.176 Å). The  $\text{Co2}$  and  $\text{Co3}$  atoms are also linked by  $\mu\text{-O}$  and  $\mu_3\text{-O}$  bridges ( $\text{Co}\cdots\text{Co}$ , 3.174 Å) (Scheme 1). All the outer EO-azido bridges are almost linear with an  $\text{N-N-N}$  of  $176.3^\circ$ , while one  $\mu_3$  site is occupied purely by azide groups ( $\text{N11}$ ) with an  $\text{N-N-N}$  angle of  $180^\circ$ . The cationic  $\text{Co}_{12}$  cluster has a disclike structure in which the cobalt centres are almost coplanar. To date, only four examples of  $\text{Co}_{12}$  clusters are known,<sup>[11a,16]</sup> and only one has a coplanar disclike structure;<sup>[16b]</sup> however, such disclike mixed-valence  $\text{Co}_{12}$  clusters containing  $\text{N}_3^-$  is unprecedented.

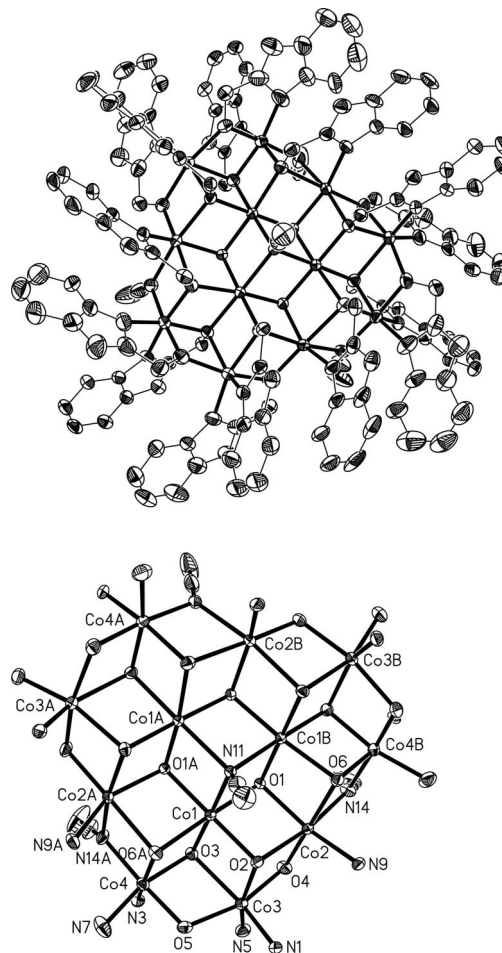


Figure 2. ORTEP drawings of the dodecanuclear cation (top) and dodecanuclear core (bottom) in **2** with ellipsoids at the 50% probability level. Symmetry codes: (a)  $-x + y, -x + 1, z$ ; (b)  $-y + 1, x - y + 1, z$ .

The magnetic properties of **1** and **2** were measured. The dc magnetic susceptibility of **1** was measured at 0.1 T from 2–300 K, as shown in Figure 3. The value of the effective magnetic moment at room temperature is  $7.21 \mu_{\text{B}}$  per  $\text{Co}_2$  unit. Upon lowering the temperature, the effective magnetic moment gradually increases because of the presence of intradimer ferromagnetic interactions. The following rapid decrease in  $\mu_{\text{eff}}$  to 2 K can be attributed to the contribution of the orbital angular momentum to the overall magnetism and/or to the zero-field splitting of  $\text{Co}^{\text{II}}$ . This behaviour is

consistent with other double EO azido-bridged dimers.<sup>[14b,17]</sup> The six-coordinate octahedral Co<sup>II</sup> complexes are known to have more complex magnetic behaviour influenced by the orbital angular momentum  $L$ . Briefly, the single-ion Co<sup>II</sup> lowest-lying atomic term  $^4F$  is split in the octahedral ligand field symmetry into three crystal-field terms  $^4T_1$ ,  $^4T_2$  and  $^4A_2$ . Only the first term is thermally populated and has a non-zero orbital angular momentum. On lowering the symmetry, the  $^4T_1$  term is further split into the  $^4A_2$  and  $^4E$  terms, separated by  $\Delta$ .<sup>[18]</sup> As a result of the heteroleptic distorted octahedral coordination sphere of the cobalt(II) central atoms of **1**, such an energy splitting is expected. The Hamiltonian shown in Equation (1) was used to describe the magnetic properties of dinuclear complex **1**.

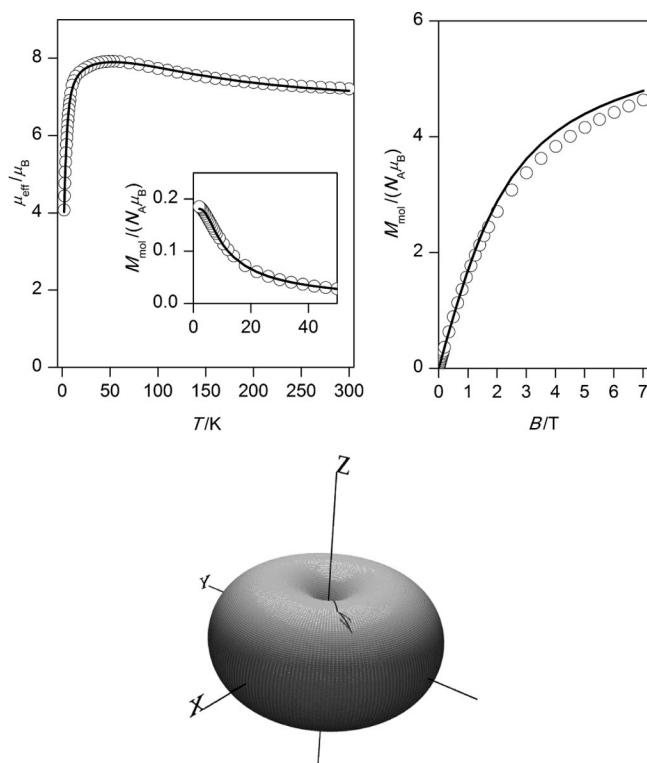


Figure 3. Top: temperature dependence of the effective magnetic moment of **1** (calculated from the magnetization at  $B = 0.1$  T), with the low-temperature region of the magnetization expanded in the inset and the field dependence of the magnetization at  $T = 2$  K. Empty circles – experimental data, full lines – calculated data with the Hamiltonian Equation (1) and  $J = +49.3$  cm<sup>-1</sup>,  $\lambda = -114$  cm<sup>-1</sup>,  $a = 1.48$ ,  $\Delta = +1215$  cm<sup>-1</sup>. Bottom: 3D diagram of the molar magnetization of **1** for different orientations of magnetic field at  $B = 7$  T and  $T = 2$  K.

$$\begin{aligned} \hat{H} = & -J(\mathbf{S}_1 \cdot \mathbf{S}_2) - a\lambda(\mathbf{S}_1 \cdot \mathbf{L}_1 + \mathbf{S}_2 \cdot \mathbf{L}_2) \\ & + \Delta(L_{z,1}^2 - L_1(L_1 + 1)/3 + L_{z,2}^2 - L_2(L_2 + 1)/3) \\ & + \mu_B \mathbf{B}(g_e \mathbf{S}_1 + g_s \mathbf{S}_2 - a\mathbf{L}_1 - a\mathbf{L}_2) \end{aligned} \quad (1)$$

where  $J$  stands for the isotropic exchange constant among the Co<sup>II</sup> centres,  $a$  is the orbital reduction factor,  $\lambda$  is spin-orbit coupling and  $g_e = 2.0023$ . The Hamiltonian was applied to the  $|M_{L,1}, M_{S,1}\rangle |M_{L,2}, M_{S,2}\rangle$  functions with  $M_{L,k} = 0, \pm 1$  and  $M_{S,k} = \pm 1/2, \pm 3/2$ . The angular orbital momen-

tum  $L$  is considered as the fictitious angular momentum,  $L = 1$ , with the effective Lande  $g$  factor,  $g_L = -a$ , because of  $T_1$ -P isomorphism.<sup>[19]</sup> As a result, there are 144 magnetic levels for the dinuclear model. The orbital reduction factor comprises two parameters,  $a = A\kappa$ , where  $A$  varies from 1 to 3/2 and results from admixture of the excited terms reflecting the ligand field strength and  $\kappa$  describes the lowering orbital contribution as a result of covalency of the metal–ligand bond and has the values  $0.70 < \kappa < 1$ . Moreover, the spin-orbit coupling parameter  $\lambda$  can also be reduced relative to its free-ion value  $\lambda_0 = -180$  cm<sup>-1</sup>, which is attributable to the covalent character of the donor–acceptor bond. There are several analytical susceptibility equations for polynuclear Co<sup>II</sup> complexes derived under various assumptions, usually by using the van Vleck equation.<sup>[20]</sup> Herein, we used a different approach based on the full diagonalization technique and numerical calculation of the energy levels and the molar magnetization as shown in Equation (2).

$$M_{\text{mol}} = N_A kT \frac{\partial \ln Z}{\partial B} \quad (2)$$

where  $Z$  is the partition function and  $B$  is magnetic field strength.<sup>[19]</sup> The overall magnetization of the system was calculated as the integral average over the different orientations of the magnetic field defined in the polar coordinates as  $\mathbf{B} = B(\sin\theta\cos\phi, \sin\theta\sin\phi, \cos\theta)$  in order to properly interpret the powder magnetic data [Equation (3)].

$$M_{\text{mol}} = 1 / 4\pi \int_0^{2\pi} \int_0^\pi M_{\text{mol}}(B) \sin\theta d\theta d\phi \quad (3)$$

The mutual fitting of the temperature and magnetic field dependences of the magnetization resulted in  $J = +49.3$  cm<sup>-1</sup>,  $\lambda = -114$  cm<sup>-1</sup>,  $a = 1.48$  and  $\Delta = +1215$  cm<sup>-1</sup> (Figure 3 top). As a consequence of the large orbital contribution and the symmetry lowering, the great magnetic anisotropy of the easy-plane type is found in **1**, which is shown in the three-dimensional diagram of the molar magnetization calculated at  $T = 2$  K and  $B = 7$  T (Figure 3 bottom). According to the modelling of the magnetic functions for mononuclear Co<sup>II</sup> complexes with a varying distortion parameter  $\Delta$  (for large ratios,  $|\Delta/\lambda| > 10$  and under the condition that  $\Delta$  is positive), the spin Hamiltonian formalism can be applied.<sup>[20c]</sup> We therefore also tried to fit the magnetic properties of **1** with a pure spin Hamiltonian containing the zero-field parameter [Equation (4)].

$$\hat{H} = -J(\mathbf{S}_1 \cdot \mathbf{S}_2) + \sum_{i=1}^2 \mathbf{S}_i \cdot \mathbf{D}_i \cdot \mathbf{S}_i + \mu_B \sum_{i=1}^2 \mathbf{B} \cdot \mathbf{g}_i \cdot \mathbf{S}_i \quad (4)$$

where  $J$  is the intradimer isotropic interaction and  $D$  represents the axial single-ion ZFS parameter. Now, the number of magnetic levels was reduced to 16 and the magnetization was calculated by using Equations (2) and (3). The resulting parameters are  $J = +39.4$  cm<sup>-1</sup>,  $g = 2.35$  and  $D = +27.2$  cm<sup>-1</sup> (Figure S2). To compare both theoretical approaches, the plots of the energy levels versus the magnetic field are presented (Figure S3), which show almost the same



behaviour. To summarize, the positive  $J$  value shows the strong intradimer ferromagnetic coupling consistent with typical double EO azido-bridged dimers,<sup>[17]</sup> and the large magnetic anisotropy of the easy-plane type is in accordance with similar Co<sup>II</sup> complexes.<sup>[21]</sup> Indeed, such type of magnetic anisotropy excludes SMM behaviour as was also confirmed by the AC susceptibility measurement where no obvious peaks in the imaginary part of the susceptibility were observed (Figure S4).

The variable-temperature dc magnetic moment of **2** (per Co<sub>12</sub> unit) was measured in the 2–300 K range in a dc magnetic field (0.1 T), which is shown in Figure 4 top. The  $\mu_{\text{eff}}$  is 14.8  $\mu_{\text{B}}$  at 300 K, which is much higher than that expected for 9 isolated spin-only  $S_i = 3/2$  Co<sup>II</sup> ions (11.62  $\mu_{\text{B}}$ , with  $g = 2.0$ ). This indicates significant orbital contributions from the distorted octahedral chromophore of Co<sup>II</sup>.<sup>[22]</sup> As  $T$  decreases, at first  $\mu_{\text{eff}}$  decreases, reaches a minimum at 35 K with  $\mu_{\text{eff}} = 14.0 \mu_{\text{B}}$ , then it increases to a maximum of 14.8  $\mu_{\text{B}}$  at 10 K. A sharp decrease follows, which might be mainly attributed to the presence of the orbital angular contribution or the ferromagnetic exchange interactions between the Co<sup>II</sup> ions. A similar magnetic behaviour has previously been observed for a Co<sub>12</sub> cluster.<sup>[11a]</sup> This behaviour is typically observed when antiferromagnetic interactions between the magnetic centres are dominant and when the ground state of the system corresponds to a ferrimagnetic arrangement of spins. The field dependence of the magnetization at low temperatures (Figure 4 top right) reveals that the magnetization reaches 19.2  $\mu_{\text{B}}$  at 7 T without true saturation. Notwithstanding a significant amount of magnetic anisotropy in this system, the ac susceptibility shows no out-of-phase signal above 1.8 K. In order to estimate the magnetic interactions in **2**, the spin Hamiltonian was postulated as shown in Equation (5).

$$\begin{aligned} \hat{H} = & -J_1(\mathbf{S}_1 \cdot \mathbf{S}_2 + \mathbf{S}_2 \cdot \mathbf{S}_3 + \mathbf{S}_3 \cdot \mathbf{S}_1) \\ & -J_2 \left( \mathbf{S}_1 \cdot \mathbf{S}_4 + \mathbf{S}_1 \cdot \mathbf{S}_8 + \mathbf{S}_1 \cdot \mathbf{S}_9 + \mathbf{S}_2 \cdot \mathbf{S}_4 + \mathbf{S}_2 \cdot \mathbf{S}_5 + \mathbf{S}_2 \cdot \mathbf{S}_6 \right. \\ & \left. + \mathbf{S}_3 \cdot \mathbf{S}_6 + \mathbf{S}_3 \cdot \mathbf{S}_7 + \mathbf{S}_3 \cdot \mathbf{S}_8 + \mathbf{S}_4 \cdot \mathbf{S}_5 + \mathbf{S}_6 \cdot \mathbf{S}_7 + \mathbf{S}_8 \cdot \mathbf{S}_9 \right) \\ & + \mu_B \sum_{i=1}^9 \mathbf{S}_i \cdot \mathbf{B} \cdot \mathbf{g}_i \end{aligned} \quad (5)$$

where  $J_1$  and  $J_2$  stand for the isotropic exchange constant among adjacent Co<sup>II</sup> centres according to Figure 4 bottom. The exchange coupling of the nine Co<sup>II</sup> centres, each with a local spin  $S_i = 3/2$ , leads to the number  $N = (2S_i + 1)^9 = 4^9 = 262\,144$  of magnetic states. The total spin ranges between  $S = 1/2$  and  $S = 27/2$ . Unfortunately, the above postulated spin Hamiltonian does not allow us to obtain an analytical formula for the energy levels. Moreover, it is not feasible to efficiently diagonalize such large interaction matrices. Provisionally, in the case of the isotropic exchange only and the under condition that all  $g$  factors are equal, the final interaction matrix expressed in the coupled basis set labelled as  $|aSM\rangle$  by using the irreducible tensor operators technique<sup>[19]</sup> ( $a$  stands for the intermediate quantum numbers denoting the coupling path) can be factorized according to the total spin  $S$ . As a result, the energies in the

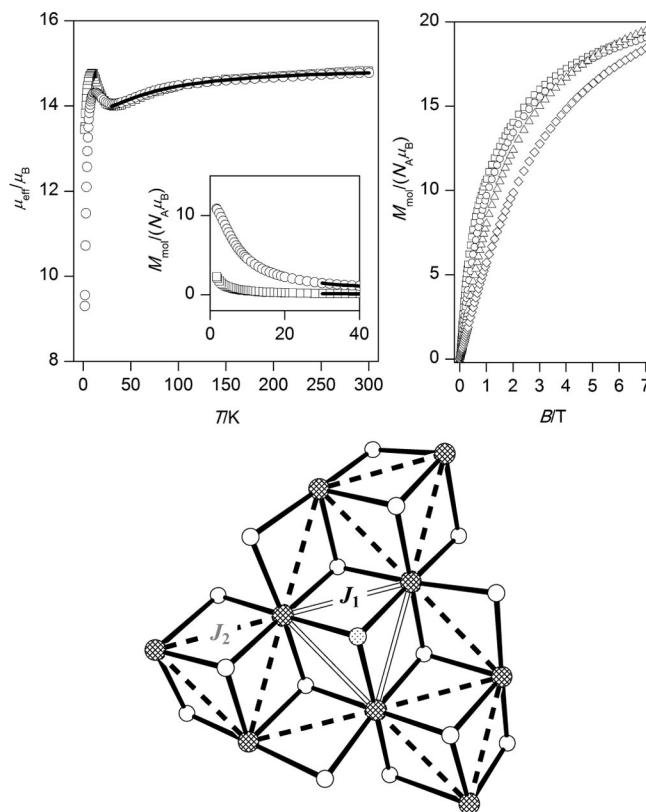


Figure 4. Top: temperature dependence of the effective magnetic moment [calculated from magnetization at  $B = 0.1$  (squares) and 1.0 T (circles)], with the low-temperature region expanded in the inset and the field dependence of the magnetization at  $T = 1.8$  (squares), 3.0 (circles), 5.0 (triangles), 8.0 K (diamonds) for **2**. Empty symbols – experimental points, lines – calculated data with the spin Hamiltonian Equation (5) and the parameters in the text. Bottom: Schematic diagram of the magnetic interactions between the magnetic centres according to the spin Hamiltonian Equation (5).

zero magnetic field are obtained. The largest dimension of the submatrix is 5300 for  $S = 7/2$  (Table S1). Consequently, the energy levels in the non-zero magnetic field are calculated as  $E_f(aSM) = E_{0,f}(aS) + \mu_B g B M$ . With the energy levels, the molar magnetization can easily be calculated from [Equation (6)].

$$M_{\text{mol}} = N_A \mu_B g \frac{\sum_j M \exp[-E_j(aSM)/kT]}{\sum_j \exp[-E_j(aSM)/kT]} \quad (6)$$

The experimental data above 30 K, which are most likely unaffected by non-isotropic terms, were subjected to the fitting procedure and the best-fit was obtained for:  $J_1 = -10.3 \text{ cm}^{-1}$ ,  $J_2 = +0.98 \text{ cm}^{-1}$ ,  $g = 2.58$ . The relatively strong antiferromagnetic coupling was found in the inner triangle mediated by the  $\mu_{1,1,1}$ -azido bridge and the  $\mu_3$ -O atoms, and, on the contrary, the ferromagnetic exchange was found in the outer shell mediated by the  $\mu_3$ -O bridges.

## Conclusions

In summary, two new cobalt clusters were synthesized from the facile reactions of  $\text{Co}(\text{NO}_3)_2$  or  $\text{Co}(\text{ClO}_4)_2$  with HL in the presence of azide. Complex **1** is a  $\mu_{1,1}$ -azido-bridged dinuclear cobalt(II) cluster, and **2** is an unusual disclike dodecanuclear  $\text{Co}^{\text{II}}_9\text{Co}^{\text{III}}_3$  cluster with three  $\mu_3\text{-O}^{2-}$ , one  $\mu_{1,1,1}\text{-N}_3^-$ , three  $\mu_{1,1}\text{-N}_3^-$ , nine  $\mu_3\text{-L}^-$  and six  $\mu\text{-L}^-$  bridges. Magnetic studies reveal that a strong ferromagnetic coupling through double EO azido bridges exists in **1**, while both ferromagnetic coupling through the  $\mu_3\text{-O}_\text{L}$  and  $\mu\text{-O}_\text{L}$  pathways and antiferromagnetic coupling through the  $\mu_{1,1,1}\text{-N}_3^-$  pathway exist in **2**, which results in a ferrimagnetic behaviour of **2**.

## Experimental Section

**Materials and Physical Measurements:** All of the starting materials employed were commercially available and used as received without further purification. The C, H, and N microanalyses were carried out with an Elementar Vario-EL CHNS elemental analyzer. The FT-IR spectra were recorded from KBr pellets in the range 4000–400  $\text{cm}^{-1}$  on a Bio-Rad FTS-7 spectrometer. Magnetic susceptibility measurements of **1** and **2** were performed on a Quantum Design MPMS-XL7 SQUID instrument. The diamagnetic correction for each sample was determined from Pascal's constant.

**Synthesis of  $[\text{Co}_2(\text{HL})_4(\text{N}_3)_2](\text{NO}_3)_2$  (**1**):** A methanol solution (10 mL) of  $\text{NaN}_3$  (0.065 g, 1.0 mol) and HL (0.074 g, 0.5 mmol) was added dropwise to a stirred methanol solution (10 mL) of  $\text{Co}(\text{NO}_3)_2 \cdot 6\text{H}_2\text{O}$  (0.145 g, 0.5 mmol), and a small amount of pink precipitate was observed. The resultant solution was filtered and left to stand at room temperature, and pink block crystals of **1** were formed (yield: 0.040 g, 35% based on HL).  $\text{C}_{32}\text{H}_{32}\text{Co}_2\text{N}_{16}\text{O}_{10}$  (**1**) (918.60): calcd. C 41.84, H 3.51, N 24.40; found C 41.75, H 3.62, N 24.31. IR (KBr, 4000–400  $\text{cm}^{-1}$ ):  $\tilde{\nu}$  = 3405 (m), 3141 (w), 2910 (vw), 1624 (m), 1504 (w), 1266 (w), 1112 (s), 1002 (w), 789 (m), 618 (m), 482 (m)  $\text{cm}^{-1}$ .

**Synthesis of  $[\text{Co}_{12}\text{O}_3(\text{N}_3)_4(\text{L})_{15}(\text{ClO}_4)_2 \cdot \text{H}_3\text{tea} \cdot 9.5\text{H}_2\text{O}$  (**2**):** A methanol solution (10 mL) of  $\text{NaN}_3$  (0.065 g, 1.0 mol), HL (0.074 g, 0.5 mmol) and  $\text{H}_3\text{tea}$  (0.015 g, 0.1 mmol) was added dropwise to a stirred methanol solution (10 mL) of  $\text{Co}(\text{ClO}_4)_2 \cdot 6\text{H}_2\text{O}$  (0.185 g, 0.5 mmol). The clear deep-brown solution was filtered and left to stand at room temperature, and deep-brown plate crystals of **2** were formed (yield: 0.082 g, 67% based on HL).  $\text{C}_{126}\text{H}_{139}\text{Cl}_2\text{Co}_{12}\text{N}_{43}\text{O}_{38.5}$  (**2**) (3649.86): calcd. C 41.46, H 3.84, N 16.50; found C 41.34, H 3.94, N 16.43. IR (KBr, 4000–400  $\text{cm}^{-1}$ ):  $\tilde{\nu}$  = 3371 (m), 3192 (w), 3056 (vw), 2911 (w), 2059 (vs), 1624 (m), 1539 (m), 1453 (vs), 1385 (w), 1334 (m), 1274 (s), 1104 (vw), 1095 (vs), 933 (w), 839 (w), 746 (vs), 618 (s), 498 (w), 447 (m)  $\text{cm}^{-1}$ .

**X-Ray Crystallographic Study:** Diffraction intensities of **1** and **2** were collected on a Bruker Apex CCD area-detector diffractometer ( $\text{Mo-K}\alpha$ ,  $\lambda$  = 0.71073 Å). Absorption corrections were applied by using the multiscan program SADABS.<sup>[23]</sup> The structures were solved with direct methods and refined with a full-matrix least-squares technique with the SHELXTL program package.<sup>[24]</sup> Anisotropic thermal parameters were applied to all non-hydrogen atoms. The organic hydrogen atoms were generated geometrically; the aqua hydrogen atoms were located from difference maps and refined with isotropic temperature factors. Crystal Data of **1** at 150(2) K:  $\text{C}_{32}\text{H}_{32}\text{Co}_2\text{N}_{16}\text{O}_{10}$ ,  $M$  = 918.60  $\text{g mol}^{-1}$ , orthorhombic, space group  $Ccca$ ,  $a$  = 15.5283(19),  $b$  = 16.132(2),  $c$  =

15.0349(17) Å,  $V$  = 3766.2(8) Å<sup>3</sup>,  $Z$  = 4,  $\rho$  = 1.620  $\text{g cm}^{-3}$ ,  $\theta_{\text{max}}$  = 25.99°, total data 5763, unique data 1774,  $\mu$  = 0.961  $\text{mm}^{-1}$ , 139 parameters,  $R_1$  = 0.0328 for  $I \geq 2\sigma(I)$  and  $wR_2$  = 0.0926 for all data. Crystal Data of **2** at 150(2) K:  $\text{C}_{126}\text{H}_{139}\text{Cl}_2\text{Co}_{12}\text{N}_{43}\text{O}_{38.5}$ ,  $M$  = 3649.86  $\text{g mol}^{-1}$ , trigonal, space group  $P\bar{3}1c$ ,  $a$  = 20.6709(7),  $c$  = 43.737(3) Å,  $V$  = 16184.4(12) Å<sup>3</sup>,  $Z$  = 4,  $\rho$  = 1.498  $\text{g cm}^{-3}$ ,  $\theta_{\text{max}}$  = 27.87°, total data 58665, unique data 11852,  $\mu$  = 1.313  $\text{mm}^{-1}$ , 688 parameters,  $R_1$  = 0.1003 for  $I \geq 2\sigma(I)$  and  $wR_2$  = 0.2935 for all data. CCDC-748741 (**1**) and -748742 (**2**) contain the supplementary crystallographic data for this paper. These data can be obtained free of charge from The Cambridge Crystallographic Data Centre via [www.ccdc.cam.ac.uk/data\\_request/cif](http://www.ccdc.cam.ac.uk/data_request/cif).

**Supporting Information** (see footnote on the first page of this article): The hydrogen-bonded architecture and the magnetic characterization of **1** are presented.

## Acknowledgments

This work was supported by the National Natural Science Foundation of China (grant nos 20525102, 90922009, 50872157 and 20821001), the “973 Project” (2007CB815305), and the Czech Ministry of Education, Youth and Sports (grant no. MSM6198959218).

- [1] D. Gatteschi, R. Sessoli, *Angew. Chem. Int. Ed.* **2003**, *42*, 268–297; a) W. Wernsdorfer, N. Aliaga-Alcalde, D. N. Hendrickson, G. Christou, *Nature* **2002**, *416*, 406–409; b) A. Author, B. Co-author, *Angew. Chem. Int. Ed.* **2006**, *45*, 1–5.
- [2] D. Gatteschi, R. Sessoli, *Angew. Chem. Int. Ed.* **2003**, *42*, 268–297.
- [3] a) M. Murugesu, W. Wernsdorfer, K. A. Abboud, G. Christou, *Angew. Chem. Int. Ed.* **2005**, *44*, 892–896; b) E. K. Berchin, *Chem. Commun.* **2005**, 5141–5153.
- [4] M. N. Leuenberge, D. Loss, *Nature* **2001**, *410*, 789–793.
- [5] M. Cavallini, J. Gomez-Segura, D. Ruiz-Molina, M. Massi, C. Albonetti, C. Rovira, J. Veciana, F. Biscarini, *Angew. Chem. Int. Ed.* **2005**, *44*, 888–892.
- [6] M. Murugesu, M. Habrych, W. Wernsdorfer, K. A. Abboud, G. Christou, *J. Am. Chem. Soc.* **2004**, *126*, 4766–4767.
- [7] A. K. Boudalis, C. P. Raptopoulou, B. Abarca, R. Ballesteros, M. Chadlaoui, J.-P. Tuchagues, A. Terzis, *Angew. Chem. Int. Ed.* **2006**, *45*, 432–435.
- [8] a) E. C. Yang, D. N. Hendrickson, W. Wernsdorfer, M. Nakano, L. N. Zakharov, R. D. Sommer, A. L. Rheingold, M. Ledezmagairaud, G. Christou, *J. Appl. Phys.* **2002**, *91*, 7382–7384; b) M. Murrie, S. J. Teat, H. Stoeckli-Evans, H. U. Güdel, *Angew. Chem. Int. Ed.* **2003**, *42*, 4653–4656; c) A. K. Boudalis, C. P. Raptopoulou, B. Abarca, R. Ballesteros, M. Chadlaoui, J. P. Tuchagues, A. Terzis, *Angew. Chem. Int. Ed.* **2006**, *45*, 432–435; d) S. J. Langley, M. Helliwell, R. Sessoli, P. Rosa, W. Wernsdorfer, R. E. P. Winpenny, *Chem. Commun.* **2005**, 5029–5031; e) A. Ferguson, A. Parkin, J. Sanchez-Benitez, K. Kamenev, W. Wernsdorfer, M. Murrie, *Chem. Commun.* **2007**, 3473–3475; f) T. Shiga, T. Matsumoto, M. Noguchi, T. Onuki, N. Hoshino, G. N. Newton, M. Nakano, H. Oshio, *Chem. Asian J.* **2009**, *4*, 1660–1663.
- [9] a) H. Oshio, M. Nakano, *Chem. Eur. J.* **2005**, *11*, 5178–5185; b) H. Oshio, N. Hoshino, T. Ito, M. Nakano, *J. Am. Chem. Soc.* **2004**, *126*, 8805–8812; c) J. Ribas-Arino, T. Baruah, M. R. Pederson, *J. Am. Chem. Soc.* **2006**, *128*, 9497–9505; d) H. Miyasaka, K. Nakata, K.-I. Sugiura, M. Yamashita, R. Clérac, *Angew. Chem. Int. Ed.* **2004**, *43*, 707–711.
- [10] a) W.-G. Wang, A.-J. Zhou, W.-X. Zhang, M.-L. Tong, X.-M. Chen, M. Nakano, C. C. Beedle, D. N. Hendrickson, *J. Am. Chem. Soc.* **2007**, *129*, 1014–1015; b) A.-J. Zhou, L.-J. Qin, C. C. Beedle, S. Ding, M. Nakano, J.-D. Leng, M.-L. Tong, D. N. Hendrickson, *Inorg. Chem.* **2007**, *46*, 8111–8113; c) A.-J.

- Zhou, J.-L. Liu, R. Herchel, J.-D. Leng, M.-L. Tong, *Dalton Trans.* **2009**, 3182–3192; d) L.-L. Fan, F.-S. Guo, L. Yun, Z.-J. Lin, R. Herchel, J.-D. Leng, Y.-C. Ou, M.-L. Tong, *Dalton Trans.* **2010**, 39, 1771–1780.
- [11] a) M.-H. Zeng, M.-X. Yao, H. Liang, W.-X. Zhang, X.-M. Chen, *Angew. Chem. Int. Ed.* **2007**, 46, 1832–1835; b) X.-Y. Song, Y.-H. Xu, L.-C. Li, D.-Z. Liao, Z.-H. Jiang, *Inorg. Chim. Acta* **2007**, 360, 2039–2044.
- [12] a) T. F. Liu, D. Fu, S. Gao, Y. Z. Zhang, H. L. Sun, G. Su, Y. Liu, *J. Am. Chem. Soc.* **2003**, 125, 13976–13977; b) G. S. Papaefstathiou, S. P. Perlepes, A. Escuer, R. Vicente, M. Font-Bardia, X. Solans, *Angew. Chem. Int. Ed.* **2001**, 40, 884–886; c) Y.-Z. Zhang, W. Wernsdorfer, F. Pan, Z.-M. Wang, S. Gao, *Chem. Commun.* **2006**, 1, 3302–3304; d) Y.-F. Zeng, X. Hu, F.-C. Liu, X.-H. Bu, *Chem. Soc. Rev.* **2009**, 38, 469–480; e) A. Escuer, G. Aromí, *Eur. J. Inorg. Chem.* **2006**, 4721–4736.
- [13] Crystal parameters for the heptanuclear Co<sub>7</sub> cluster: trigonal, space group *R*-3 (no. 148), *a* = 19.728(5), *c* = 26.754(11) Å, *V* = 9017(5) Å<sup>3</sup>, *Z* = 3.
- [14] a) M. G. B. Drewa, C. J. Hardingb, J. Nelsonb, *Inorg. Chim. Acta* **1996**, 246, 73–79; b) X.-N. Cheng, W.-X. Zhang, X.-M. Chen, *J. Am. Chem. Soc.* **2007**, 129, 15738–15739.
- [15] W. Liu, H. H. Thorp, *Inorg. Chem.* **1993**, 32, 4102–4105.
- [16] a) L. Stuart, H. Madeleine, S. Roberta, J. T. Simon, E. P. W. Richard, *Inorg. Chem.* **2008**, 47, 497–507; b) C. William, C. D. Garner, M. H. Al-Samman, *Inorg. Chem.* **1983**, 22, 1534–1538; c) E. K. Brechin, O. Cador, A. Caneschi, C. Cadiou, S. G. Harris, S. Parsons, M. Vancib, R. E. P. Winpenny, *Chem. Commun.* **2002**, 1860–1861.
- [17] a) H.-Z. Kou, S. Hishiyama, O. Sato, *Inorg. Chim. Acta* **2008**, 361, 2396–2406; b) M. G. B. Drewa, C. J. Hardingb, J. Nelsonb, *Inorg. Chim. Acta* **1996**, 246, 73–79.
- [18] a) B. N. Figgis, M. A. Hitchman, *Ligand Field Theory and Its Applications*, Wiley-VCH, **2000**; b) M. E. Lines, *J. Chem. Phys.* **1971**, 55, 2977–2984.
- [19] R. Boča, *Theoretical Foundations of Molecular Magnetism*, Elsevier, Amsterdam, **1999**.
- [20] a) H. Sakiyama, R. Ito, H. Kumagai, K. Inoue, M. Sakamoto, Y. Nishida, M. Yamasaki, *Eur. J. Inorg. Chem.* **2001**, 2027–2032; b) H. Sakiyama, *Inorg. Chim. Acta* **2006**, 359, 2097–2100; c) F. Lloret, M. Julve, J. Cano, R. Ruiz-Garcia, E. Pardo, *Inorg. Chim. Acta* **2008**, 361, 3432–3445 and references cited therein.
- [21] R. Boča, *Coord. Chem. Rev.* **2004**, 248, 757–815.
- [22] O. Kahn, *Molecular Magnetism*, VCH, Weinheim, **1993**.
- [23] G. M. Sheldrick, *SADABS 2.05*, University of Göttingen, Göttingen, Germany, **2002**.
- [24] *SHELXTL 6.10*, Bruker Analytical Instrumentation, Madison, Wisconsin, USA, **2000**.

Received: February 24, 2010  
Published Online: April 14, 2010